Theoretical study of the electronic structure of the Sr_2 molecule

N. Boutassetta, A. R. Allouche, and M. Aubert-Frécon
Laboratoire de Spectrométrie Ionique et Moléculaire, CNRS et Université Lyon I, Campus de la Doua, Bâtiment 205, F69622 Villeurbanne Cedex, France
(Received 13 November 1995)

The electronic structure of the Sr_2 molecule has been investigated by use of a two-valence-electron pseudopotential, configuration-interaction calculations with the four active electrons via the CIPSI (configuration interaction by perturbation of a multiconfiguration wave function selected iteratively) algorithm, and addition of a core-polarization potential. Potential-energy curves for the ground and 21 excited states of Sr_2 as well as for the ground state of Sr_2^+ have been determined, and subsequent spectroscopic constants have been obtained. Quite a good agreement with the few available experimental values is displayed for the unambiguously assigned states $X\ ^1\Sigma_g^+$, $A\ ^1\Sigma_u^+$ of Sr_2 and $X\ ^2\Sigma_u^+$ of Sr_2^+, while present predictions lead to a different assignment for the observed $B\ ^1\Pi_u$ state which is found to correspond to the adiabatic $(3)^1\Pi_u$ state.

PACS number(s): 31.10.+z

I. INTRODUCTION

Spectroscopy of alkaline-earth dimers attracts special interest due to the different structure between their van der Waals ground state with a large equilibrium distance and quite strongly bound excited states at significantly smaller internuclear distances. Among these molecules, little has been known up to now about the Sr_2 molecule. Four states have been investigated experimentally. One state, assigned to $^1\Sigma_u^+$ was characterized from matrix isolation spectroscopy [1,2], experiments which first proved the existence of stable Sr_2 molecules. The ground state $X\ ^1\Sigma_g^+$ and the excited state $A\ ^1\Sigma_u^+$ have been characterized through the analysis of laser-induced fluorescence spectra of the molecule produced in a heat pipe oven [3,4]. The $B\ ^1\Pi_u$ state has been investigated recently from depletion spectroscopy on Sr_2 molecules produced in a seeded molecular beam [5]. On the theoretical side, Sr_2 has only been studied from density-functional methods [6,7], providing predictions of the binding energy somewhat larger than the experimental value.

Here we present a theoretical investigation of the electronic structure of Sr_2 using a different approach, based on valence-electron pseudopotentials, the configuration interaction (CI) for four active electrons, and the addition of core-polarization potentials. This method is very similar to one we used previously for investigations of the electronic structure of barium compounds BaH [8], BaLi [9], BaNa [10], BaK [11], and Ba_2 [12]. Predictions obtained in that way for BaH are in good quantitative agreement with accurate experimental data for equilibrium distances R_e, transition energies T_e, and vibrational constants ω_e, with discrepancies $\Delta R_e < 0.04$ Å, $\Delta T_e < 200\ cm^{-1}$, and $\Delta\omega_e < 40\ cm^{-1}$. For BaLi, our predictions, which were used as a guide for experimentalists, agree well with corresponding experimental values for the three states observed up to now: $X\ ^2\Sigma^+$, $(2)^2\Sigma^+$ and $(2)^2\Pi$ with $\Delta R_e < 0.05$ Å and $\Delta T_e < 300\ cm^{-1}$.

After a summary of the method used in Sec. II, potential-energy curves and spectroscopic constants for 22 molecular states of Sr_2 are reported in Sec. III. Present data might be useful to experimentalists involved in spectroscopic investigations of this molecule, or interested in atomic collision processes such as energy pooling [13,14].

II. METHOD

The strontium atom has been treated through a two-electron semiempirical pseudopotential taken from Fuentealba *et al.* [15]:

$$V_{\rm ps}^{\rm Sr} = -\frac{Z}{r} + \sum_{l=0} B_l^{\rm Sr} \exp(-\beta_l^{\rm Sr} r^2) \mathbf{P}_l^{\rm Sr}, \tag{1}$$

where $\mathbf{P}_l^{\rm Sr} = \Sigma_m |lm\rangle_{\rm Sr}\langle lm|_{\rm Sr}$ is the projection operator on symmetry l with respect to the core Sr, and Z is the core charge. The parameters $B_l^{\rm Sr}$ and $\beta_l^{\rm Sr}$ fitted to experimental data are available in Ref. [15] for $l=0$, 1, and 2.

A Gaussian basis set $(5s5p6d1f/5s5p3d1f)$ has been determined, which is suited to reproduce the $5s$, $4d$, $5p$, and $6s$ orbitals using the preceding pseudopotential. The f orbital has been included to improve the description of the $5s4d\ ^{1,3}D$ states of Sr. The basis set is displayed in Table I.

At the CI level, Sr is treated as a two-valence-electron system, and no explicit account for correlation between core and valence electrons is taken. Fuentealba *et al.* introduced the interaction between polarizable cores and the valence electrons by adding a semiempirical polarization potential to the two-valence-electron pseudopotential. Such a description, pseudopotential plus core-polarization potential, was seen to provide an accurate value for the bond distance of the ground-state hydride SrH [16]. In the present work, we use such a core-polarization potential in order to bring in some core effects, core polarization and core-valence correlation, via the Foucrault-Millié-Daudey form [17]:

$$V_{\rm cpp} = -\tfrac{1}{2} \sum_{X=A,B} \alpha_X \mathbf{f}_X \cdot \mathbf{f}_X, \tag{2}$$

where A and B denote the two Sr atoms and α_X is the dipole polarizability of the core X. The electric field $\mathbf{f}_X$ created on

TABLE I. Gaussian basis sets for Sr.

	Two-electron pseudopotential calculations		Ten-electron pseudopotential calculations	
Orbitals	Exponents	Contraction coefficients	Exponents	Contraction coefficients
s	0.791 740	1.0	5.879 157	0.196 709
	0.316 178	1.0	3.092 482	−0.625 898
	0.066 565	1.0	0.644 667	0.735 723
	0.026 990	1.0	0.298 876	1.0
	0.013 495	1.0	0.057 276	1.0
			0.023 870	1.0
			0.011 935	1.0
p	0.225 825	1.0	2.432 472	−0.374 899
	0.095 691	1.0	1.664 234	0.387 615
	0.042 077	1.0	0.569 989	0.655 838
	0.018 077	1.0	0.220 718	1.0
	0.009 038 5	1.0	0.067 629	1.0
			0.026 727	1.0
			0.013 363	1.0
d	3.618 081	−0.007 501	3.618 081	−0.007 501
	0.996 656	0.108 098	0.996 656	0.108 098
	0.390 735	0.278 540	0.390 735	0.278 540
	0.122 770	0.477 318	0.122 770	0.477 318
	0.036 655	1.0	0.036 655	1.0
	0.018 327	1.0	0.018 327	1.0
f	0.1	1.0	0.1	1.0

0

X by valence electrons and other cores is modified by a cutoff function *F* acting on the electronic part,

$$\mathbf{f}_X=\sum_{i=1}^{2}\frac{\mathbf{r}_{iX}}{r_{iX}^3}F(r_{iX},\rho_X)-\sum_{X'\neq X}\frac{\mathbf{R}_{X'X}}{R_{X'X}^3}Z_{X'}, \qquad (3)$$

where $\mathbf{r}_{iX}$ describes the valence-electron–core relative positions, and $\mathbf{R}_{X'X}$ describes the core-core relative positions. The cutoff function is expanded as follows:

$$F(r_{iX},\rho_X)=\sum_{l}\sum_{m=-l}^{l}F_l(r_{iX},\rho_X^l)|lm\rangle_X\langle lm|_X, \qquad (4)$$

TABLE II. Ionization energies for Sr^+, transition energies and ionization potential for Sr, calculated with two effective core potentials (values in cm^{-1}, cutoff radii ρ^l in a_0). Δ is the difference between experimental energy and calculated energy.

		Ten-electron pseudopotential $\rho^0=1.248\,847$, $\rho^1=1.447\,745$, $\rho^2=\rho^3=2.121\,131$		Two-electron pseudopotential $\rho^0=2.089\,30$, $\rho^1=2.117\,00$, $\rho^2=\rho^3=1.644\,71$	
Level	Experimental energies	Calculated energies	Δ	Calculated energies	Δ
Sr^+ $5s\ ^2S$	88 964	88 964	0	88 964	0
$4d\ ^2D$	74 239.9	74 239.8	0	74 239.8	0
$5p\ ^2P$	64 714.51	64 714.5	0	64 714.4	0
$6s\ ^2S$	41 227.47	41 133	94	41 167	60
$5d\ ^2D$	35 625.7	35 093	533	35 222	404
$6p\ ^2P$	33 002.17	32 887	115	32 981	21
Sr $5s^2\ ^1S$	0	0		0	
$5p5p\ ^3P$	14 711.73	14 673	39	14 548	163
$5s4d\ ^3D$	18 259.53	18 375	115	18 242	17
$5s4d\ ^1D$	20 149.7	20 524	374	20 209	60
$5s5p\ ^1P$	21 698.5	21 731	33	21 459	240
Ionization energy	45 925.6	45 839	87	46 070	144

TABLE III. Comparison between energies at large R ($R=100a_0$) and experimental atomic transition energies (in cm^{-1}).

Dissociation	Experimental [a] values	Calculated [b] values	Molecular states
$Sr(5s^2\,{}^1S)+Sr(5s^2\,{}^1S)$	0	0	$^1\Sigma_g^+$
		0	
$Sr(5s5p\,{}^3P)+Sr(5s^2\,{}^1S)$	14 711.73	14 541	$^3\Sigma_{g,u}^+, ^3\Pi_{g,u}$
		14 587	
$Sr(5s4d\,{}^3D)+Sr(5s^2\,{}^1S)$	18 259.53	18 289	$^3\Sigma_{g,u}^+, ^3\Pi_{g,u}, ^3\Delta_{g,u}$
		18 183	
$Sr(5s4d\,{}^1D)+Sr(5s^2\,{}^1S)$	20 149.7	20 676	$^1\Sigma_{g,u}^+, ^1\Pi_{g,u}, ^1\Delta_{g,u}$
		20 341	
$Sr(5s5p\,{}^1P)+Sr(5s^2\,{}^1S)$	21 698.5	21 966	$^1\Sigma_{g,u}^+, ^1\Pi_{g,u}$
		21 731	

[a]From Ref. [19], values averaged over J.

[b]First line: ten-electron pseudopotential. Second line: two-electron pseudopotential.

where $F_l(r_{iX},\rho_X^l)$ is defined by

$$F_l(r_{iX},\rho_X^l)=0 \quad \text{for } r_{iX}<\rho_X^l$$
$$=1 \quad \text{for } r_{iX}\geqslant\rho_X^l.$$

l-dependent cutoff functions $F_l(r_{iX},\rho_X^l)$ are introduced to account for the fact that valence electrons interact differently with cores depending on their angular symmetry l.

For α we used the theoretical value [18] $\alpha=5.51a_0^3$ previously used by Fuentealba *et al.*, while the ρ_X^l parameters have been fitted to reproduce experimental energies [19] (averaged over J) for the states $5s\ {}^2S$, $4d\ {}^2D$, and $5p\ {}^2P$ of Sr^+. Their values are reported in Table II. They have been used to calculate ionization energies for Sr^+, and transition energies and ionization potential for Sr with a full valence

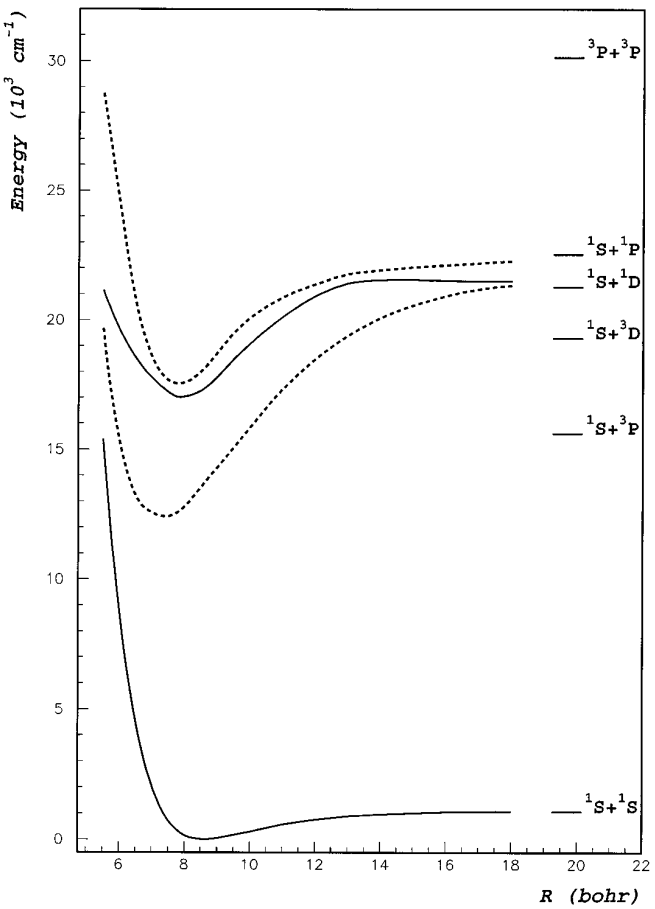

FIG. 1. Potential-energy curves for the $^1\Sigma^+$ states. Full lines: $^1\Sigma_g^+$; dashed lines: $^1\Sigma_u^+$.

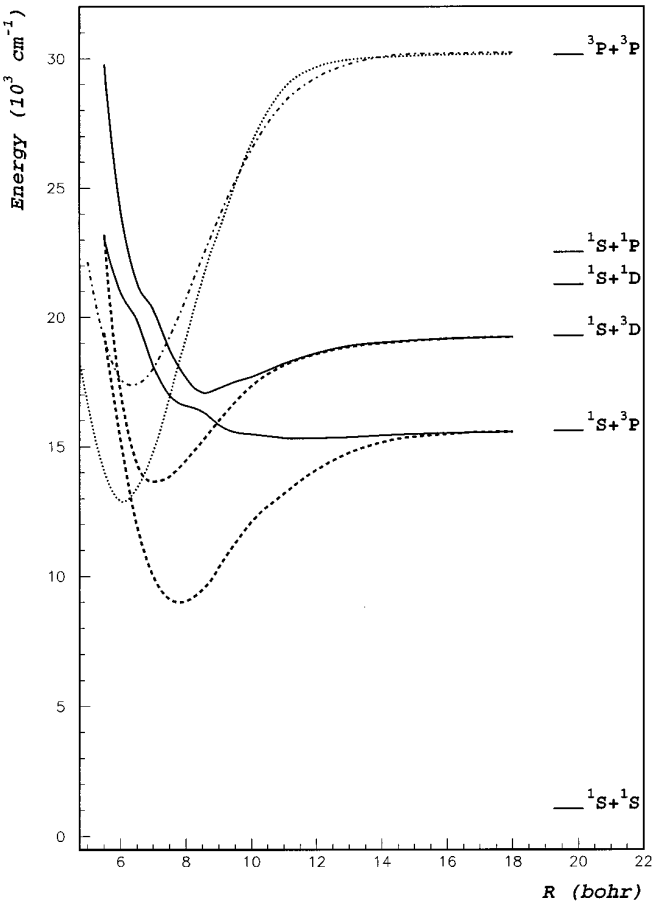

FIG. 2. Potential-energy curves for the $^3\Sigma^{+/-}$ and $^5\Sigma^-$ states. Full lines: $^3\Sigma_g^+$; dashed lines: $^3\Sigma_u^+$; dotted line: $^3\Sigma_g^-$; -·-·-·: $^5\Sigma_u^-$.

CI. Due to the fitting procedure to determine ρ^0, ρ^1, and ρ^2, the states $5s\ ^2S$, $4d\ ^2D$, and $5p\ ^2P$ of Sr^+ are reproduced exactly. For the transition energies of Sr and for the levels of Sr^+ not included in the fitting procedure for the ρ^l, an accurate description is provided. A good agreement with corresponding experimental data is displayed, with a maximum deviation of $\sim 240\ cm^{-1}$ for the level $5s5p\ ^1P$ of Sr and of $\sim 400\ cm^{-1}$ for the level $5d\ ^2D$ of Sr^+.

It should be noted that, in analogy with our previous work on Ba_2 [12], we also described Sr through a ten-electron quasirelativistic nonempirical effective core potential determined by Kaupp *et al.* [16] in the form given by Eq. (1). A Gaussian basis set $(7s7p6d1f/5s5p3d1f)$ displayed in Table I was used. At the CI level, Sr was treated as a two-electron system by freezing the $4s$ and $4p$ orbitals, and a core-polarization potential similar to that used for the two-electron pseudopotential approach was determined. Corresponding fitted parameters are displayed in Table II together with the so-calculated (full valence CI) values for ionization energies in Sr^+, and transition energies and ionization potential for Sr. As can be seen, the agreement with experimental data is somewhat less good than that obtained using the two-electron pseudopotential.

The molecule Sr_2 is treated as a four-electron system even when considering the ten-electron pseudopotential by freezing the orbitals $4s$ and $4p$. Core effects are taken into account at the molecular level through the core-polarization potentials determined for Sr. Configuration-interaction calculations for the four active electrons have been performed through the three class CIPSI algorithm (configuration interaction by perturbation of a multiconfiguration wave function selected iteratively) [20,21]. Two subspaces S and M with $S \subset M$ are treated variationally. Their sizes are defined by the following thresholds: $\eta_S = 0.013$ and $\eta_M = 0.002$ for calculations with a ten-electron pseudopotential, and $\eta_S = 0.03$ and $\eta_M = 0.0025$ for calculations with a two-electron pseudopotential. The simply and doubly excited determinants (with respect to those of the S subspace) not included in M constitute the third subspace R, which is treated by perturbation.

III. RESULTS

The $^{2S+1}\Lambda_{g,u}^{(+/-)}$ states dissociating into the five lowest limits Sr $(5s^2\ ^1S)$ + Sr $(5s^2\ ^1S;\ 5s5p\ ^3P;5s4d\ ^3D;$ $5s4d\ ^1D;5s5p\ ^1P)$ plus the states $^{3,5}\Sigma_{g,u}^-$ and $(3)^1\Pi_u$ dissociating into Sr$(5s5p\ ^3P)$ + Sr $(5s5p\ ^3P)$ have been investigated in the range of internuclear distances $5.0 \leqslant R \leqslant 18.0 a_0$. In order to assess the accuracy of our approach, we have performed calculations at a very large distance $R = 100 a_0$. The calculated energies are compared to the experimental atomic transition energies in Table III. As already observed for the description of excited states of Sr and Sr^+, the agreement is better for the semiempirical two-electron pseudopotential approach than for the nonempirical ten-electron one, with a maximum deviation of $\sim 200\ cm^{-1}$ for the states dissociating into Sr $(5s^2\ ^1S)$ + Sr $(5s4d\ ^1D)$. Because a ten-valence-electron pseudopotential treatment of the Sr_2 molecule would be much more expensive than a two-valence-electron pseudopotential one, while results in this limiting case are not better, we decided to perform all molecular calculations with the simplest pseudopotential.

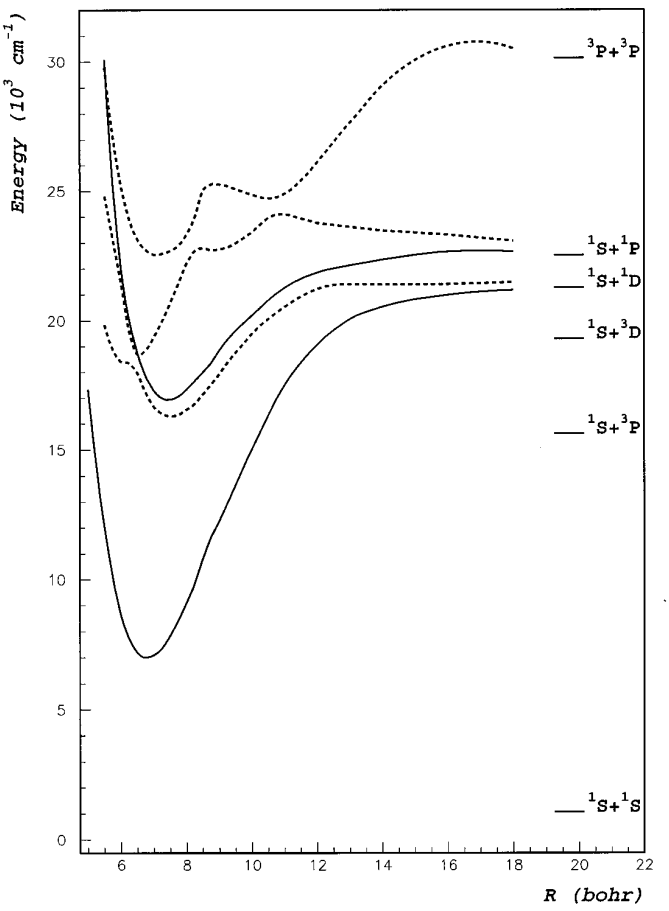

FIG. 3. Potential-energy curves for the $^1\Pi$ states. Full lines: $^1\Pi_g$; dashed lines: $^1\Pi_u$.

Potential-energy curves are drawn in Figs. 1–5 for the $^1\Sigma$, $^{3,5}\Sigma$, $^1\Pi$, $^3\Pi$, and $^{1,3}\Delta$ states, respectively. If they are smooth with a well-defined unique minimum for the species $^1\Sigma_{g,u}^+$, $^3\Sigma_u^+$, $^3\Sigma_g^-$, $^5\Sigma_u^-$, $^{1,3}\Pi_g$, $^1\Delta_{g,u}$, and $^3\Delta_u$, they are more complex for the species $^3\Sigma_g^+$, $^{1,3}\Pi_u$, and $^3\Delta_g$, for which they present various avoided crossings.

From the calculated adiabatic energies, values for the minimum-to-minimum electronic excitation energy T_e, the equilibrium internuclear distance R_e, the harmonic frequency ω_e, and the rotational constant B_e have been calculated for bound states. For states with a unique minimum, all calculated values were used in these determinations, while for states with several minima such as the $(2)^3\Sigma_g^+$, $(1)^3\Delta_g$, (1) and $(2)^3\Pi_u$, and (1), (2), and $(3)^1\Pi_u$ states, only energy values in the range of R restricted to the lowest minimum were taken into account. Calculated spectroscopic constants are displayed in Table IV together with previous experimental and theoretical data.

The ground state is calculated to be weakly bound $(D_e = 1088\ cm^{-1})$ at rather large internuclear distance $(R_e = 4.531\ Å)$ and with a small harmonic frequency $(\omega_e = 43\ cm^{-1})$, corresponding to a van der Waals structure. Its CI wave function displays a simple configuration closed-shell structure, with a calculated weight at $R = 8 a_0$ of

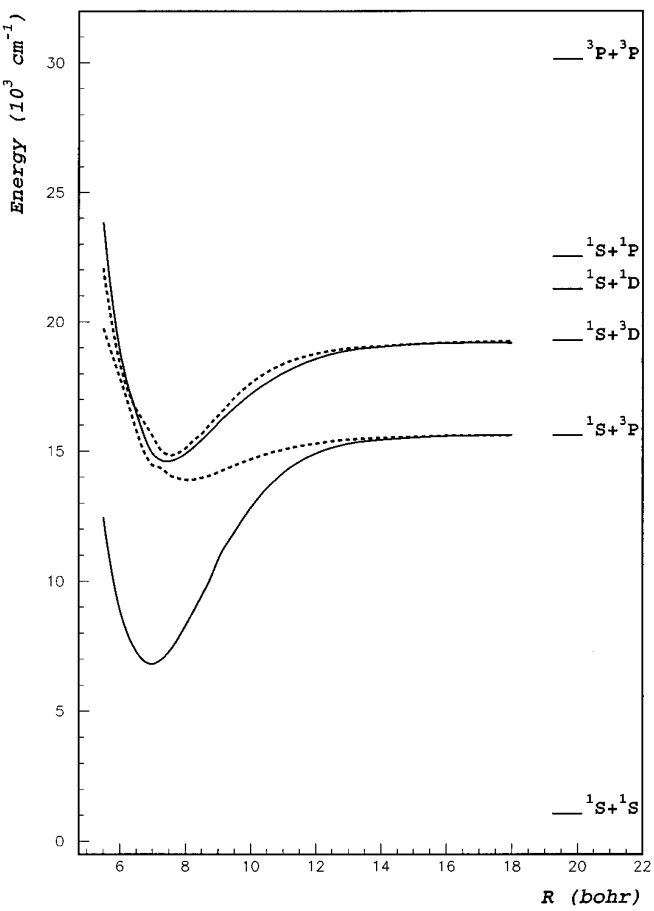

FIG. 4. Potential-energy curves for the $^3\Pi$ states. Full lines: $^3\Pi_g$; dashed lines: $^3\Pi_u$.

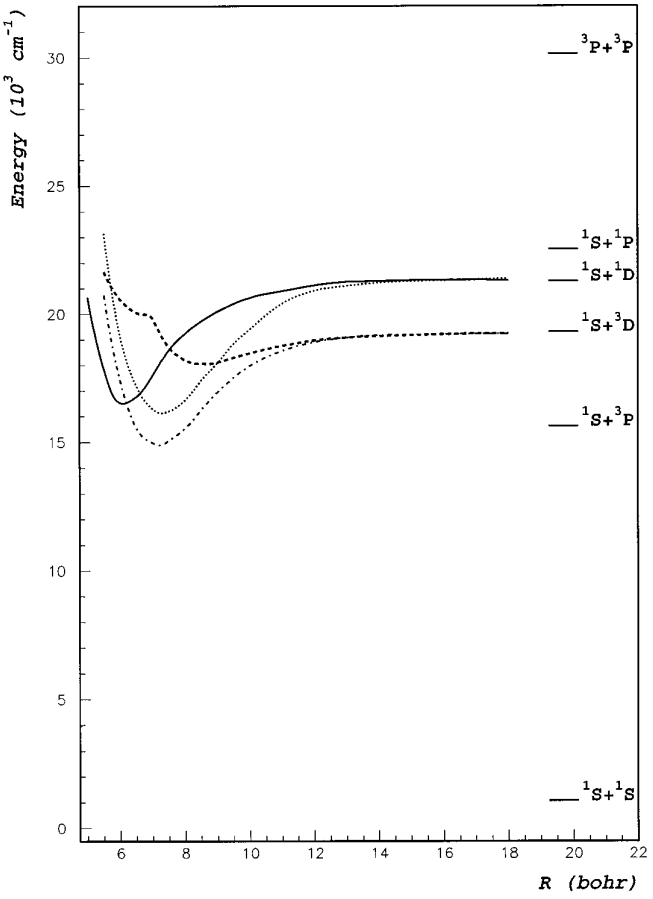

FIG. 5. Potential-energy curves for the $^{1,3}\Delta$ states. Full line: $^1\Delta_g$; dotted line: $^1\Delta_u$; dashed line: $^3\Delta_g$; -·-·-·: $^3\Delta_u$.

~ 0.95 for the configuration $\sigma_g^2\sigma_u^2$ where σ_g and σ_u are valence molecular orbitals (MO's). Calculated spectroscopic constants are in quite good agreement with the corresponding experimental values [4] obtained from the analysis of laser-induced fluorescence series $D_e = 1060 \pm 30$ cm^{-1}, $R_e = 4.446$ Å, and $\omega_e = 40.32 \pm 0.02$ cm^{-1}. The binding energy is accurately reproduced, while a relative difference δ of $\sim 2\%$ is obtained for R_e and $\delta \sim 7\%$ for ω_e.

Present results are also compared in Table IV with previously available theoretical results from density-functional calculations. The earlier values were obtained from local spin-density-functional calculations [6], while the more recent calculations included gradient corrections to the local-density approximation [7]. Our predictions are seen to be in better agreement with experiment, especially for the binding energy. As a matter of fact, it has already been pointed out for other homonuclear dimers of group IIA [7] that density-functional approaches provide overestimated values for the binding energy. The only previous results we knew for excited states are also due to density-functional calculations [6]. It should be noted that they predict the same order as present results for the four lowest excited states, while values for spectroscopic constants are significantly different.

From Figs. 1–5, it can be seen that the relatively flat potential-energy curve of the ground state is very different from the potential curves of the excited states, which present generally larger binding energies and smaller equilibrium distances. In order to discuss the nature of these excited states, we performed a theoretical investigation of the ground state of Sr_2^+, for which, to the best of our knowledge, there exist no previous theoretical data. We used basically the method described in Sec. II and treated Sr_2^+ as a three-electron molecule at the CI level with the CIPSI algorithm. The calculated potential-energy curve of the $X\ ^2\Sigma_u^+$ state of Sr_2^+ is drawn in Fig. 6. Calculated spectroscopic constants are $T_e = 37\,983$ cm^{-1}, $\omega_e = 81$ cm^{-1}, $D_e = 9065$ cm^{-1}, and $R_e = 4.104$ Å, to be compared to the following experimental values deduced from an investigation of the ground state of Sr_2^+ related to the spectroscopy of small Sr_n clusters [22]: $T_e = 38180 \pm 100$ cm^{-1}, $\omega_e = 86 \pm 3$ cm^{-1}, and $D_e = 8800 \pm 100$ cm^{-1}.

Various excited states with equilibrium distance ~ 4 Å may be understood as resulting from a Sr_2^+ ground state plus a simply excited electron. This is illustrated in Fig. 6, in which the potential curves for the states $(2)^1\Sigma_u^+$, $(1)^3\Sigma_u^+$, $(2)^3\Sigma_u^+$, $(1)^1\Delta_u$, and $(1)^3\Delta_u$ are drawn together with the curve for the $X\ ^2\Sigma_u^+$ state of Sr_2^+. Furthermore, the weights of the simple excitations from the lowest valence MO's σ_g and σ_u occupied in the $X\ ^1\Sigma_g^+$ state to the two lowest virtual MO's $\phi_{g,u}^*$ and $\phi_{g,u}^{**}$ are important, and generally dominant, in the wave functions of these states. For instance, at $R = 8a_0$, these weights ω are 0.54 and 0.30 for the excitations $\sigma_u \rightarrow \sigma_g^*$ and $\sigma_u \rightarrow \sigma_g^{**}$, respectively, for the $(2)^1\Sigma_u^+$, and for the state $(1)^1\Delta_u$; $\omega = 0.70$ and 0.55 for the excitations $\sigma_u \rightarrow \delta_g^*$ and $\sigma_u \rightarrow \delta_g^{**}$, respectively.

TABLE IV. Spectroscopic constants for the $^{2S+1}\Lambda_{g,u}^{(+/-)}$ states of Sr_2.

State		T_e (cm^{-1})	ω_e (cm^{-1})	R_e (Å)	$10B_e$ (cm^{-1})
$X\ ^1\Sigma_g^+$		0	43	4.531	0.187
	Gerber, Möller, and Schneider [a]	0	40.32 ± 0.02	4.446	0.194
	Jones [b]	0	45	4.81	
	Ortiz-Ballone [c]	0	47.6	4.503	
$(1)^3\Pi_g$		6844	97	3.684	0.283
$(1)^1\Pi_g$		7041	101	3.588	0.299
$(1)^3\Sigma_u^+$		8992	83	4.124	0.226
$(1)^1\Sigma_u^+$		12 363	79	3.850	0.259
$(1)^3\Sigma_g^-$		12 926	125	3.228	0.369
$(2)^3\Sigma_u^+$		13 614	96	3.744	0.274
$(1)^3\Pi_u$		13 890	54	4.320	0.206
$(2)^3\Pi_g$		14 573	90	3.946	0.247
$(2)^3\Pi_u$		14 883	90	4.037	0.236
$(1)^3\Delta_u$		14 900	84	3.778	0.269
$(1)^1\Delta_u$		16 158	82	3.868	0.257
$(1)^1\Pi_u$		16 243	96	3.952	0.246
$(1)^1\Delta_g$		16 425	124	3.251	0.364
$(2)^1\Pi_g$		17 004	84	3.969	0.244
$(2)^1\Sigma_g^+$		17 024	69	4.213	0.217
$(2)^3\Sigma_g^+$		17 101	81	4.545	0.186
$(1)^5\Sigma_u^-$		17 383	100	3.363	0.340
$(2)^1\Sigma_u^+$		17 541	83	4.099	0.229
	Gerber, Möller, and Schneider [a]	$17\,357.9\pm0.2$	85.07 ± 0.34	3.952	0.2456
$(1)^3\Delta_g$		17 991	66	4.473	0.192
$(2)^1\Pi_u$		18 714	176	3.487	0.316
$(3)^1\Pi_u$		22 548	76	3.797	0.267
	Bordas *et al.* [d]	$22\,173\pm10$	80.4 ± 1.0	3.85 ± 0.05	

[a]Reference [4].
[b]Reference [6].
[c]Reference [7].
[d]Reference [5].

As previously pointed out for Ba_2 [12], some of the excited states of Sr_2 considered here with smaller values of the equilibrium distance ($\sim$3.5 Å) and larger values of ω_e exhibit a doubly excited character, while quite less pronounced than for Ba_2. For instance, it is the case for the $(1)^1\Delta_g$ state, in the wave function of which the double excitation $\sigma_u^2 \rightarrow \pi_{ux}^{*2} - \pi_{uy}^{*2}$ has a weight of 0.44. The $(1)^3\Sigma_g^-$ and $(1)^5\Sigma_u^-$ states which dissociate adiabatically to the limit Sr $(5s5p\ ^3P)$+Sr $(5s5p\ ^3P)$ also have this double character. The $(1)^3\Sigma_g^-$ state is dominated by the configuration $\sigma_u^2 \rightarrow \pi_{ux}^{*2} + \pi_{uy}^{*2}$ ($\omega = 0.64$), while the configurations $\sigma_u\sigma_g \rightarrow \pi_{ux}^{*2} + \pi_{uy}^{*2}$ ($\omega = 0.49$), $\pi_u^*\pi_u^{**}$ ($\omega = 0.33$) are predominant for the state $(1)^5\Sigma_u^-$.

Apart from the ground state, we knew experimental values of spectroscopic constants only for three states, namely the $A\ ^1\Sigma_u^+$ and the $B\ ^1\Pi_u$ states investigated in the gas phase, and for one state $^1\Sigma_u^+$ investigated from matrix spectroscopy. The $A\ ^1\Sigma_u^+ \leftarrow X\ ^1\Sigma_g^+$ system has been investigated from laser-induced fluorescence of the Sr_2 molecule produced in a heat pipe oven [3,4]. Calculated results for the $A\ ^1\Sigma_u^+$ state which dissociates adiabatically to Sr $(5s^2\ ^1S)$+Sr $(5s5p\ ^1P)$ are seen to be in quite good agreement with experiment with $\Delta T_e \sim 200$ cm^{-1}, $\Delta\omega_e = 2$ cm^{-1}, and $\Delta R_e = 0.147$ Å.

A structured absorption band was observed for Sr_2 in rare-gas matrices [1] at 710 nm in the Ar matrix ($T_e = 13\,805$ cm^{-1} and $\omega_e = 66$ cm^{-1}), and at 730 nm in the Kr matrix ($T_e = 13\,426$ cm^{-1} and $\omega_e = 68$ cm^{-1}). It was assumed to correspond to the electronic transition $^1\Sigma_u^+[^1S+^1P] \leftarrow X\ ^1\Sigma_g^+$. In fact, its characteristics are seen to be closer to that calculated for the $(1)^3\Pi_u[^1S+^3P]$ state with $\Delta T_e < 100$ cm^{-1} and $\Delta\omega_e = 14$ cm^{-1}, which might be the electronic state observed.

The excited state $B\ ^1\Pi_u$ of Sr_2 has been characterized from depletion spectroscopy, and experimental spectroscopic constants have been obtained [5]. Experimental values $T_e = 22\,173\pm10$ cm^{-1}, $\omega_e = 80.4\pm1.0$ cm^{-1}, and $R_e = 3.85\pm0.05$ Å are seen to be in quite good agreement with those calculated for the inner well of the $(3)^1\Pi_u$ adiabatic state which correlates adiabatically to the doubly excited limit Sr $(5s5p\ ^3P)$+Sr $(5s5p\ ^3P)$. The differences are $\Delta T_e < 400$ cm^{-1}, $\Delta\omega_e < 5$ cm^{-1}, and $\Delta R_e \sim 0.05$ Å. It should be noted that the calculated adiabatic potential-energy curves for the states $^1\Pi_u$ (see Fig. 3) present various obvious

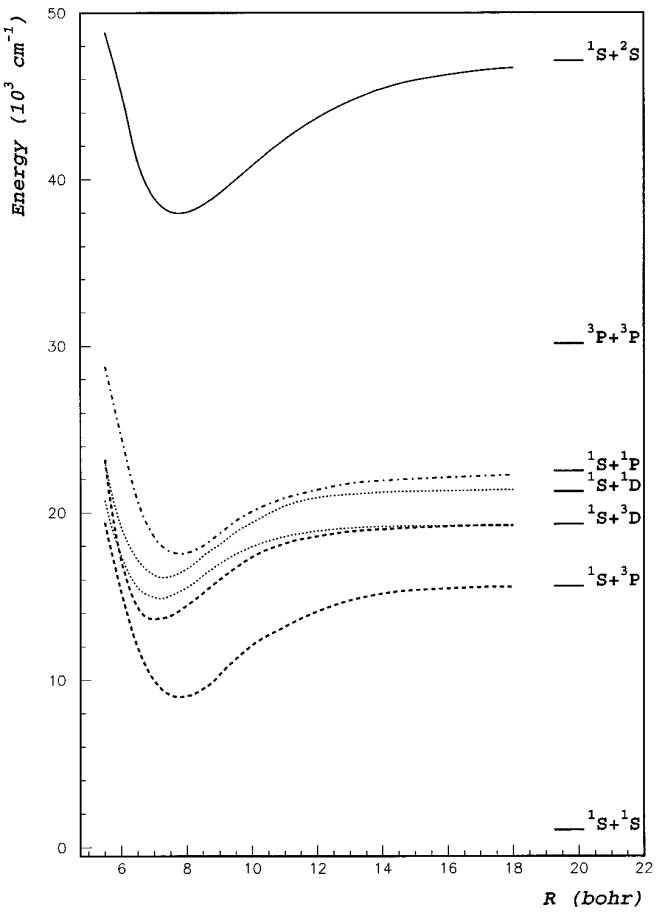

FIG. 6. Comparison between the potential-energy curves of the $X\ ^2\Sigma_u^+$ state of Sr_2^+ and of some excited states of Sr_2. Full line: $X\ ^2\Sigma_u^+$; dashed lines: $^3\Sigma_u^+$; dotted lines: $^{1,3}\Delta_u$; -·-·-·: $(2)^1\Sigma_u^+$.

avoided crossings. Present values for the spectroscopic constants have been obtained for the well presenting the lowest minima of each curve. The experimentally observed $B\ ^1\Pi_u$ state was assigned as the $(2)^1\Pi_u$ state dissociating into Sr $(5s^2\ ^1S)$+Sr $(5s5p\ ^1P)$. The calculated characteristics of the inner well of the $(2)^1\Pi_u$ state, i.e., $T_e=18\,714$ cm^{-1}, $\omega_e=176$ cm^{-1}, and $R_e=3.487$ Å are too far from the experimental values, so that we believe that the $^1\Pi_u$ state observed is more likely the $(3)^1\Pi_u$ state. We have calculated the dipole moment M for the transition $(3)^1\Pi_u \leftarrow X\ ^1\Sigma_g^+$. Its square M^2 presents a maximum ($\sim$10 a.u.) for a value of R very close to the R_e value ($\sim 7a_0$) of the inner well of the $(3)^1\Pi_u$ state, and decreases sharply to a small value ($\sim$0.3 a.u.) at $R\sim 8a_0$, a distance around which an avoided crossing with the adiabatic $(2)^1\Pi_u$ state takes place. Furthermore, for such a distance, the energy of the $(3)^1\Pi_u$ state is calculated to be 770 cm$-$1 above the bottom of the potential well. These two points are consistent with the fact that the highest vibrational level measured experimentally was about 700 cm^{-1} above the bottom of the potential well.

IV. CONCLUSION

Potential-energy curves and spectroscopic constants have been predicted for 22 molecular states $^{2S+1}\Lambda_{g,u}^{(+/-)}$ of the Sr_2 molecule by using a semiempirical two-valence-electron pseudopotential for Sr, treating the correlation for the four active electrons by configuration interaction through the CIPSI algorithm, and introducing a core-polarization potential. Predictions for the ground state which may be described as a weakly bound van der Waals system are seen to be in quite good agreement with experimental data, significantly better than the only previous results from density-functional calculations especially for the binding energy.

We knew only three excited states that have been investigated experimentally, i.e., two states assigned as $^1\Sigma_u^+$ and one state $^1\Pi_u$. Among these states, present predictions confirm the assignment of the $A\ ^1\Sigma_u^+$ state, and enable us to propose a different attribution for the $^1\Sigma_u^+$ state observed in rare-gas matrices and for the $B\ ^1\Pi_u$ state. Assuming present assignments, our predictions are seen to be in quite good agreement with experimental data. In a way very similar to that used for Sr_2, the potential-energy curve and corresponding spectroscopic constants have been obtained for the ground state $X\ ^2\Sigma_u^+$ of Sr_2^+, and they are seen to be quite close to the corresponding experimental values.

[1] J. C. Miller, B. S. Ault, and L. Andrews, J. Chem. Phys. **67**, 2478 (1977).
[2] J. C. Miller and L. Andrews, J. Chem. Phys. **69**, 936 (1978).
[3] T. Bergeman and P. F. Lias, J. Chem. Phys. **72**, 886 (1980).
[4] G. Gerber, R. Möller, and H. Schneider, J. Chem. Phys. **81**, 1538 (1984).
[5] C. Bordas, M. Broyer, J. Chevaleyre, and Ph. Dugourd, Chem. Phys. Lett. **197**, 562 (1992).
[6] R. O. Jones, J. Chem. Phys. **71**, 1300 (1979).
[7] G. Ortiz and P. Ballone, Phys. Rev. B **43**, 6376 (1991).
[8] A. R. Allouche, G. Nicolas, J. C. Barthelat, and F. Spiegelmann, J. Chem. Phys. **96**, 7646 (1992).
[9] A. R. Allouche and M. Aubert-Frécon, J. Chem. Phys. **100**, 938 (1994).
[10] N. Boutassetta, A. R. Allouche, and M. Aubert-Frécon, Chem. Phys. **189**, 33 (1994).
[11] N. Boutassetta, A. R. Allouche, and M. Aubert-Frécon, Chem. Phys. **201**, 393 (1995).
[12] A. R. Allouche, M. Aubert-Frécon, G. Nicolas, and F. Spiegelmann, Chem. Phys. **200**, 63 (1995).
[13] J. F. Kelly, M. Harris, and A. Gallagher, Phys. Rev. A **38**, 1225 (1988).
[14] H. G. C. Werij, M. Harris, J. Copper, and A. Gallagher, Phys. Rev. A **43**, 2237 (1991).
[15] P. Fuentealba, O. Reyes, H. Stoll, and H. Preuss, J. Chem. Phys. **87**, 5338 (1987).
[16] M. Kaupp, P. v. R. Schleyer, H. Stoll, and H. Preuss, J. Chem. Phys. **94**, 1360 (1991).

[17] M. Foucrault, Ph. Millié, and J. P. Daudey, J. Chem. Phys. **96**, 1257 (1992).
[18] P. C. Schmidt, A. Weiss, and T. P. Das, Phys. Rev. B **19**, 5525 (1979).
[19] C. E. Moore, *Atomic Energy Levels*, Natl. Bur. Stand. (U.S.) Circ. No. 467 (U.S., GPO, Washington, D.C., 1958).
[20] B. Huron, P. Rancurel, and J. P. Malrieu, J. Chem. Phys. **58**, 5475 (1973).
[21] S. Evangelisti, J. P. Daudey, and J. P. Malrieu, Chem. Phys. **75**, 95 (1983).
[22] Ph. Dugourd, J. Chevaleyre, C. Bordas, and M. Broyer, Chem. Phys. Lett. **193**, 539 (1992).